PNAS RESEARCH ARTICLE | BIOCHEMISTRY

USP11 promotes prostate cancer progression by up-regulating AR and c-Myc activity

Majid Pornour[a,b], Hee-Young Jeon[a,b], Hyunju Ryu[a,b], Sudeep Khadka[a,b], Rui Xu[a,c], Hegang Chen[d], Arif Hussain[a,b,e], Hung-Ming Lam[f], Zhihao Zhuang[g], Htoo Zarni Oo[h], Martin Gleave[h], Xuesen Dong[h], Qianben Wang[i], Christopher Barbieri[j], and Jianfei Qi[a,b,1]

Edited by Myles Brown, Dana-Farber Cancer Institute, Boston, MA; received February 16, 2024; accepted July 1, 2024

Androgen receptor (AR) is a main driver for castration-resistant prostate cancer (CRPC). c-Myc is an oncogene underlying prostate tumorigenesis. Here, we find that the deubiquitinase USP11 targets both AR and c-Myc in prostate cancer (PCa). USP11 expression was up-regulated in metastatic PCa and CRPC. USP11 knockdown (KD) significantly inhibited PCa cell growth. Our RNA-seq studies revealed AR and c-Myc as the top transcription factors altered after USP11 KD. ChIP-seq analysis showed that either USP11 KD or replacement of endogenous USP11 with a catalytic-inactive USP11 mutant significantly decreased chromatin binding by AR and c-Myc. We find that USP11 employs two mechanisms to up-regulate AR and c-Myc levels: namely, deubiquitination of AR and c-Myc proteins to increase their stability and deubiquitination of H2A-K119Ub, a repressive histone mark, on promoters of AR and c-Myc genes to increase their transcription. AR and c-Myc reexpression in USP11-KD PCa cells partly rescued cell growth defects. Thus, our studies reveal a tumor-promoting role for USP11 in aggressive PCa through upregulation of AR and c-Myc activities and support USP11 as a potential target against PCa.

AR | c-Myc | ubiquitination | gene expression | prostate cancer

Significance

Androgen receptor (AR) and c-Myc are the key transcription factors driving prostate cancer (PCa) progression. In this study, we identified the deubiquitinase USP11 as a key regulator for both AR and c-Myc. Our study revealed mechanisms by which USP11 up-regulates levels and activities of AR and c-Myc. We showed that USP11 plays a tumor-promoting role in aggressive PCa through its effect on AR and c-Myc. Thus, our study suggests that USP11 may be a target for potential PCa therapy.

Prostate cancer (PCa) is the second most common cancer in men worldwide, and metastatic castration-resistant PCa (CRPC) is the main cause of death for PCa patients. Androgen deprivation therapy (ADT), which suppresses androgen receptor (AR) activity, is the first-line treatment for metastatic PCa. However, despite initial clinical remission after ADT, the disease invariably reoccurs in 2 to 3 y and progresses to a lethal CRPC stage. The major driver for relapse is reactivation of AR transcriptional activity via multiple mechanisms, such as AR overexpression/mutation/splicing, overexpression of AR cofactors, and intratumoral androgen biosynthesis (1). Currently, the main CRPC therapies include taxane-based chemotherapy (docetaxel or cabazitaxel) and second-generation AR pathway inhibitors (enzalutamide or abiraterone). These treatments can extend survival, but CRPC eventually becomes drug resistant, driven by reactivated AR signaling (2). c-Myc is an oncogene in many cancer types and is overexpressed in human PCa tissues (3). C-Myc overexpression in the mouse prostate induces PCa development (4) and also contributes to CRPC progression (5–7).

Ubiquitination and deubiquitination play key roles in reversible regulation of protein stability. Several ubiquitin ligases induce ubiquitination and subsequent degradation of AR or c-Myc protein, while several deubiquitinases target and stabilize AR (8–10) or c-Myc (11). In this study, we found that the deubiquitinase USP11 deubiquitinates both AR and c-Myc and plays a tumor-promoting role in PCa. USP11 reportedly deubiquitinates and stabilizes several substrate proteins (12) and is known to deubiquitinate Histone H2A monoubiquitinated at K119 (hereafter called H2A-Ub), a repressive histone mark, to enhance gene expression (13). USP11 plays a tumor-promoting role in several cancer types (14–18). For example, USP11 promotes growth and metastasis of colorectal cancer by deubiquitinating and stabilizing PPP1CA (16). USP11 promotes proliferation and metastasis of hepatocellular carcinoma cells by deubiquitinating and stabilizing E2F1 (19), and USP11 promotes invasion and metastasis of ovarian cancer by deubiquitinating and stabilizing the transcription factor Snail (20). In contrast, one study has reported that USP11 deubiquitinates and stabilizes the tumor suppressor PTEN in PCa (21).

Here, we showed that USP11 knockdown (KD) inhibits PCa cell growth, regardless of PTEN status, suggesting that USP11 may promote PCa growth by targeting other substrates. Accordingly, we revealed an oncogenic role for USP11 in aggressive PCa through AR and c-Myc upregulation. Thus, our study supports the idea that USP11 may serve as a therapeutic target for aggressive PCa.

Author affiliations: [a]Department of Biochemistry and Molecular Biology, University of Maryland, Baltimore, MD 21201; [b]Marlene and Stewart Greenebaum Comprehensive Cancer Center, Baltimore, MD 21201; [c]Department of Marine Biotechnology, Institute of Marine and Environmental Technology, University of Maryland, Baltimore, MD 21202; [d]Department of Epidemiology and Public Health, University of Maryland, Baltimore, MD 21201; [e]Baltimore Veterans Affairs Medical Center, Baltimore, MD 21201; [f]Department of Urology, University of Washington, Seattle, WA 98195; [g]Department of Chemistry and Biochemistry, University of Delaware, Newark, DE 19716; [h]Department of Urologic Sciences, Vancouver Prostate Centre, University of British Columbia, Vancouver, BC V6H 3Z6, Canada; [i]Department of Pathology and Duke Cancer Institute, Duke University School of Medicine, Durham, NC 27710; and [j]Department of Urology, Weill Cornell Medical College, Cornell University, New York, NY 10065

Author contributions: M.P., H.-Y.J., H.R., and J.Q. designed research; M.P., H.-Y.J., H.R., and J.Q. performed research; A.H., H.-M.L., Z.Z., H.Z.O., M.G., X.D., Q.W., and C.B. contributed new reagents/analytic tools; M.P., H.-Y.J., S.K., R.X., H.C., and H.Z.O. analyzed data; and M.P., A.H., and J.Q. wrote the paper.

The authors declare no competing interest.

This article is a PNAS Direct Submission.

[1]To whom correspondence may be addressed. Email: jqi@som.umaryland.edu.

This article contains supporting information online at https://www.pnas.org/lookup/suppl/doi:10.1073/pnas.2403331121/-/DCSupplemental.

Published July 25, 2024.

Results

USP11 Plays a Tumor-Promoting Role in PCa. To examine the role of USP11 in more aggressive forms of PCa, we investigated USP11 transcript levels in primary versus more advanced forms of PCa. In two GEO datasets, we observed USP11 mRNA upregulation in metastatic PCa or CRPC relative to primary PCa (Fig. 1 *A* and *B*). In one TCGA PCa dataset, PCa samples were defined as USP11-high and USP11-low groups based on USP11 mRNA levels, and the USP11-high group showed a trend for shorter disease-free survival (DFS) than the USP11-low group (Fig. 1*C*, $P = 0.085$). Moreover, in three PCa datasets, 10 to 17% of metastatic PCa samples showed USP11 gene amplification (Fig. 1*D*). We evaluated the USP11 expression in PCa tissue using USP11 immunohistochemistry (IHC) staining. We first validated the USP11 antibody by showing that it detected a single distinct band in western blot analysis of PCa cells (*SI Appendix*, Fig. S1*A*) and strongly stained PCa tissue section in contrast to negative staining of adjacent tissue section by control IgG (*SI Appendix*, Fig. S1*B*). Then we performed USP11 IHC staining in PCa tissue microarrays (TMAs) and observed similar low USP11 staining in benign prostate tissues and primary PCa (Fig. 1 *E* and *F*). We observed higher levels of USP11 staining in PCa tissues after ADT, but these differences did not differ significantly from those seen among primary PCa samples (Fig. 1 *E* and *F*). By contrast, relative to primary PCa, metastatic PCa, CPRC, or neuroendocrine PCa (NEPC) showed significantly higher levels of USP11 staining (Fig. 1 *E* and *F*). In addition, human PCa cell lines showed higher levels of USP11 mRNA and protein than did normal human prostate epithelial cells (HPrECs) (*SI Appendix*, Fig. S1 *C* and *D*). These results confirm upregulation of USP11 mRNA and protein in aggressive forms of PCa.

To assess USP11 function in PCa, we used three different shRNAs to knock down USP11 in Rv1 (Fig. 1*G*), DU145 (Fig. 1*H*), or VCaP (Fig. 1*I*) cells, which we then analyzed via colony formation assays. USP11 KD significantly decreased the colony formation by these PCa cells (Fig. 1 *J* and *K*). All three USP11 shRNAs showed comparable inhibitory effects on colony formation (Fig. 1 *J* and *K*). USP11 KD significantly inhibited growth of xenograft tumors formed by Rv1, C4-2, or PC3 cells (Fig. 1 *L* and *M* and *SI Appendix*, Fig. S1 *E* and *F*). These results support a tumor-promoting role for USP11 in PCa cells.

PTEN is reportedly a USP11 substrate in PCa (21). In VCaP cells, we found that USP11 KD decreased PTEN levels and increased levels of phospho-AKT (Fig. 1*I*), consistent with the report of PTEN as a USP11 substrate. However, in Rv1 or DU145 cells, USP11 KD had no effect on levels of PTEN or phospho-AKT (Fig. 1 *G* and *H*), indicating that USP11 effects on PTEN depend on cell type. On the other hand, USP11 KD inhibited growth of PCa cells that express PTEN (Rv1, DU145, and VCaP) and of PCa cells that do not (C4-2 and PC3) (Fig. 1 *J*–*M* and *SI Appendix*, Fig. S1 *G* and *H*). These findings indicate that USP11 KD inhibits PCa cell growth regardless of PTEN status and suggest that USP11 targets other substrate(s) to promote PCa cell growth.

USP11 Is a Key Regulator of AR and c-Myc in PCa. To define pathways regulated by USP11 in PCa cells, we knocked down USP11 in Rv1 cells and performed RNA-seq analyses (22). RNA-seq confirmed efficient USP11 KD (>95% KD) (*SI Appendix*, Fig. S2*A*). Overall, USP11 KD decreased levels of 2,930 RNAs (log2 [fold change] < −0.5, *P*adj < 0.05, Fig. 2*A*, blue color) and up-regulated levels of 2,406 RNAs (log2 [fold change] > 0.5, *P*adj < 0.05, Fig. 2*A*, red color) (*SI Appendix*, Table S1). Bioinformatic analysis of down-regulated genes (log2 [fold change] < −0.9, *P*adj < 0.05) using various algorithms in Erichr indicated that the top altered GO pathways were associated with Myc, Estrogen responses or Androgen responses (Fig. 2*B*), and transcription factor analysis identified AR or MYC as the top transcription factors altered by USP11 KD. Specifically, algorithms such as ARCHS4 and Trust Transcription Factor 2019 predicted AR as the top transcription factor (Fig. 2*C* and *SI Appendix*, Fig. S2*B*), while ChEA 2022 and ENCODE predicted MYC or MAX, which heterodimerize to regulate gene expression, as the top transcription factors (Fig. 2*D* and *SI Appendix*, Fig. S2*C*). In addition, to predict USP11-regulated transcription factors, we subjected genes down-regulated by USP11 KD (log2[fold change] < −0.9, *P*adj < 0.05) to BART (binding analysis for regulation of transcription) analysis, an algorithm that predicts key transcriptional regulators underlying altered gene expression, and found MAX, ERG, and MYC to be the most significant transcription regulators altered by USP11 KD (*SI Appendix*, Fig. S2*D*). To confirm these results, we performed GSEA analysis of differentially expressed genes (DEGs) after USP11 KD and observed enrichment of AR or MYC target genes (Fig. 2*E*). In GSEA analysis of DEGs against the PID pathway database (196 gene sets), the AR pathway ranked first, and the c-Myc pathway ranked sixth (*SI Appendix*, Fig. S2*E*). Thus, the GSEA analysis also supports a key role for USP11 in regulation of AR and MYC pathways. Accordingly, RNA-seq analysis showed that USP11 KD decreased c-Myc (77% inhibition) and AR (43% inhibition) transcript levels (*SI Appendix*, Fig. S2 *F* and *G*), indicating that USP11 promotes their expression. Following RNA-seq analysis of USP11-KD cells, heatmaps indicated downregulation of AR and example AR target genes (Fig. 2*F*) and of c-Myc and example c-Myc target genes (Fig. 2*G*).

As validation, we then performed real-time RT-PCR analysis on various USP11-KD PCa lines using two different shRNAs (Fig. 2*H*). USP11 KD in AR-positive Rv1, C4-2, or VCaP cells decreased AR mRNA levels (Fig. 2*I*), while USP11 KD decreased c-Myc transcript levels both in these lines and in AR-negative DU145 cells (Fig. 2*J*). Consistently, USP11 KD in five PCa lines decreased AR and/or c-Myc protein levels (Fig. 1 *G*–*I* and *SI Appendix*, Fig. S1 *E* and *F*). USP11 KD also reduced transcript levels of the AR targets KLK2, KLK3, NKX3-1, TMPRSS2, SLC45A3, and PMEPA1 in Rv1 (*SI Appendix*, Fig. S2*H*), VCaP (*SI Appendix*, Fig. S2*I*), and C4-2 (*SI Appendix*, Fig. S2*J*) cells, and in Rv1 cells decreased those levels in the presence or absence of androgen (*SI Appendix*, Fig. S2*K*). Similarly, USP11 KD decreased levels of the c-Myc target genes MCM3, CDC6, CCNE2, MKI67, and CDK4 in Rv1 (*SI Appendix*, Fig. S2*L*), VCaP (*SI Appendix*, Fig. S2*M*), C4-2 (*SI Appendix*, Fig. S2*N*), and DU145 (*SI Appendix*, Fig. S2*O*) cells.

To evaluate the potential relevance of these in vitro findings to PCa tissues, we analyzed and correlated USP11 transcript levels with those of AR or c-Myc in human PCa datasets. In two GEO datasets, levels of USP11 and AR, but not c-Myc, were increased relative to primary PCa in both metastatic PCa (Figs. 1*A* and 2*K* and *SI Appendix*, Fig. S2*P*) and CRPC (Figs. 1*B* and 2*L* and *SI Appendix*, Fig. S2*Q*). Similarly, mRNA levels of USP11 and AR (Fig. 2*M*), but not c-Myc (*SI Appendix*, Fig. S2*R*), correlated positively with each other in a TCGA PCa dataset. Moreover, in that dataset, USP11 mRNA levels were positively correlated with target gene signatures of both AR (Fig. 2*N*) and MYC (Fig. 2*O*). Thus, overall, in PCa tissues, USP11 mRNA levels correlate positively with transcript levels of AR and both AR and MYC target genes but not with c-Myc mRNA levels.

USP11 KD Decreases Genome-Wide AR and c-Myc Binding. To determine whether USP11 loss alters binding of AR or c-Myc to chromatin, we knocked down USP11 in Rv1 cells and performed

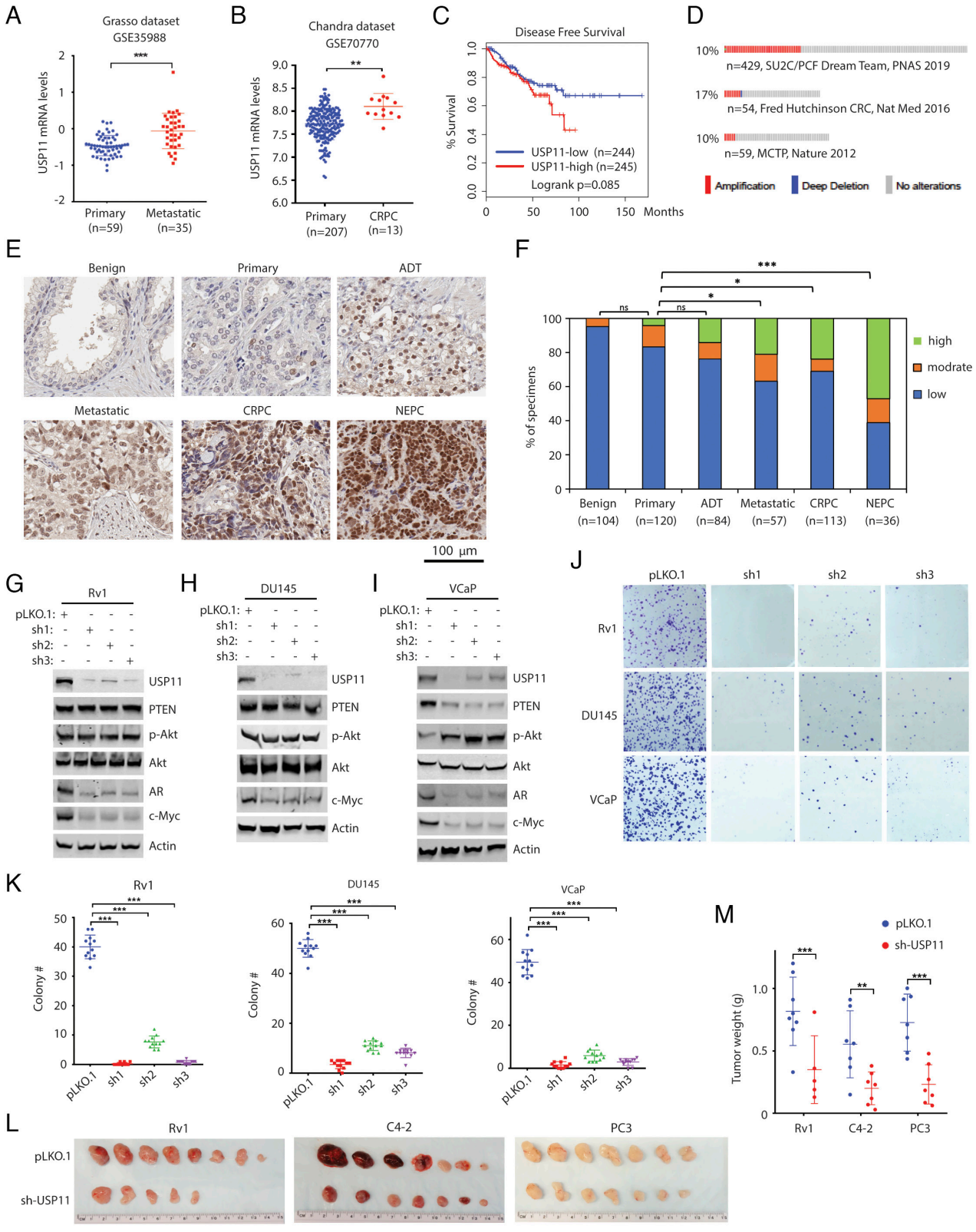

Fig. 1. (*A* and *B*) Upregulation of USP11 mRNA in metastatic PCa (*A*) or CPRC (*B*) relative to primary PCa. (*C*) Patients whose PCa samples express high USP11 transcript levels exhibit shorter survival than those expressing low levels. Survival analysis using the TCGA PCa dataset was performed using the GEPIA2 web server. (*D*) USP11 gene amplification in three PCa datasets. (*E* and *F*) Increased USP11 staining in metastatic PCa, CRPC, and NEPC specimens relative to primary PCa. Shown is representative USP11 staining of indicated PCa samples (*E*): USP11, brown; nuclei, blue. Percentage of PCa tissues displaying a given USP11 staining pattern (low, moderate, or high) in each PCa group is shown (*F*). (*G–I*) Effect of USP11 KD with three different shRNAs on PTEN and phospho-AKT levels in Rv1 (*G*), DU145 (*H*), or VCaP (*I*) cells. (*J* and *K*) USP11 KD with three different shRNAs significantly inhibits PCa cell colony formation. Indicated cells were seeded at low density and maintained for 2 wk. Colony numbers were scored in 12 high-power fields. Images represent four high-power fields. Shown are colony formation images (*J*) and quantification of colony number in indicated PCa cells (*K*). (*L* and *M*) USP11 KD inhibits xenograft tumor growth by Rv1, C4-2, and PC3 cells. Indicated cells were subcutaneously injected into athymic nude mice. Xenograft tumors were collected 4 to 5 wk later (*L*), and tumor weight was quantified (*M*).

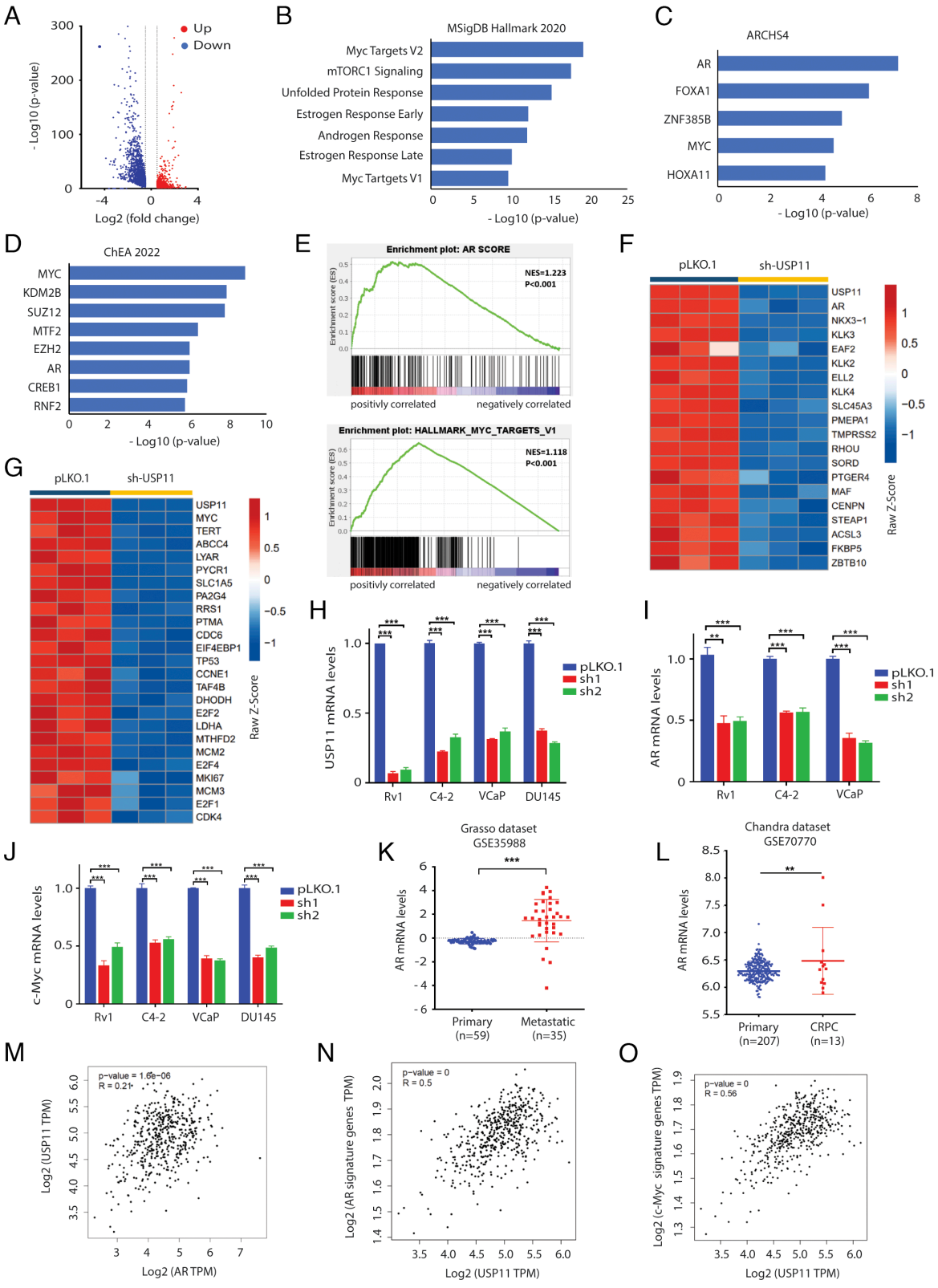

Fig. 2. (*A*) Volcano plot showing DEGs identified by RNA-seq of control and USP11-KD Rv1 cells. (*B*) GO analysis of genes down-regulated after USP11 KD was performed using the Enrichr web server. Shown are results of GO pathway analysis based on the MSigDB hallmark gene set. (*C*) ARCHS4 algorithm shows the AR target genes as the top signature altered after USP11 KD. (*D*) ChEA 2022 algorithm shows the MYC target genes as the top signature altered after USP11 KD. (*E*) GSEA analysis of DEGs after USP11 KD for enrichment of AR (*Upper* panel) or Myc (*Lower* panel) target genes. (*F* and *G*) Heatmaps showing decreased expression of classic AR (*F*) or c-Myc (*G*) targets based on RNA-seq of USP11-KD Rv1 cells. FPKM values of RNA-seq results were log2-transformed and used for heatmap preparation using the pheatmap package in R. (*H*) qRT-PCR results showing the USP11 KD in indicated PCa cells using two different USP11 shRNAs. (*I* and *J*) qRT-PCR results showing reduced AR (*I*) or c-Myc (*J*) transcript levels after USP11 KD in indicated PCa cells. (*K* and *L*) Upregulation of AR mRNA in metastatic PCa (*K*) or CRPC (*L*) relative to primary PCa. (*M*–*O*) Positive correlation of USP11 mRNA levels with levels of AR mRNA (*M*), AR target signatures (*N*), or Myc target signatures (*O*) in the TCGA PCa dataset (n = 492). Pearson correlation analysis was performed using the GEPIA2 web server.

CUT&RUN ChIP-seq analysis of AR and c-Myc (23). For AR CUT&RUN ChIP-seq, we detected 19,001 AR peaks using an AR but not IgG antibody in control cells (Fig. 3*A*). Homer motif analysis of AR peaks revealed significant enrichment of androgen-response elements (AREs) or AR half-site motifs (Fig. 3*B*). ~48% of CUT&RUN AR peaks overlap with the traditional AR ChIP-seq peaks from a published dataset of Rv1 cells (*SI Appendix*, Fig. S3*A*). These results validate our AR CUT&RUN ChIP-seq studies. USP11 KD reduced the global AR peaks (Fig. 3*A*). Among the AR peaks, ~58% (11,060 of 19,001) showed a statistically significant reduction in size after USP11 KD, while 42% (7,951 of 19,001) showed reductions in peak size that were not significant (Fig. 3 *C* and *D*). The distribution of AR peaks across distinct chromosomal locations, such as promoters and intergenic regions, was notably altered by USP11 KD (Fig. 3*E*). For examples, USP11 KD decreased AR peak signals on the KLK3 enhancer, KLK2 promoter, and TMPRSS2 promoter/enhancer (Fig. 3*F*).

For c-Myc CUT&RUN ChIP-seq, we identified 15,157 peaks using a c-Myc antibody relative to control IgG in control cells (Fig. 3*G*). Homer motif analysis of those peaks revealed significant enrichment of MYC binding motifs (Fig. 3*H*). ~82% of CUT&RUN c-Myc peaks overlap with the traditional c-Myc ChIP-seq peaks from a published dataset of Rv1 cells (*SI Appendix*, Fig. S3*B*). These results again validate our CUT&RUN c-Myc ChIP-seq studies. USP11

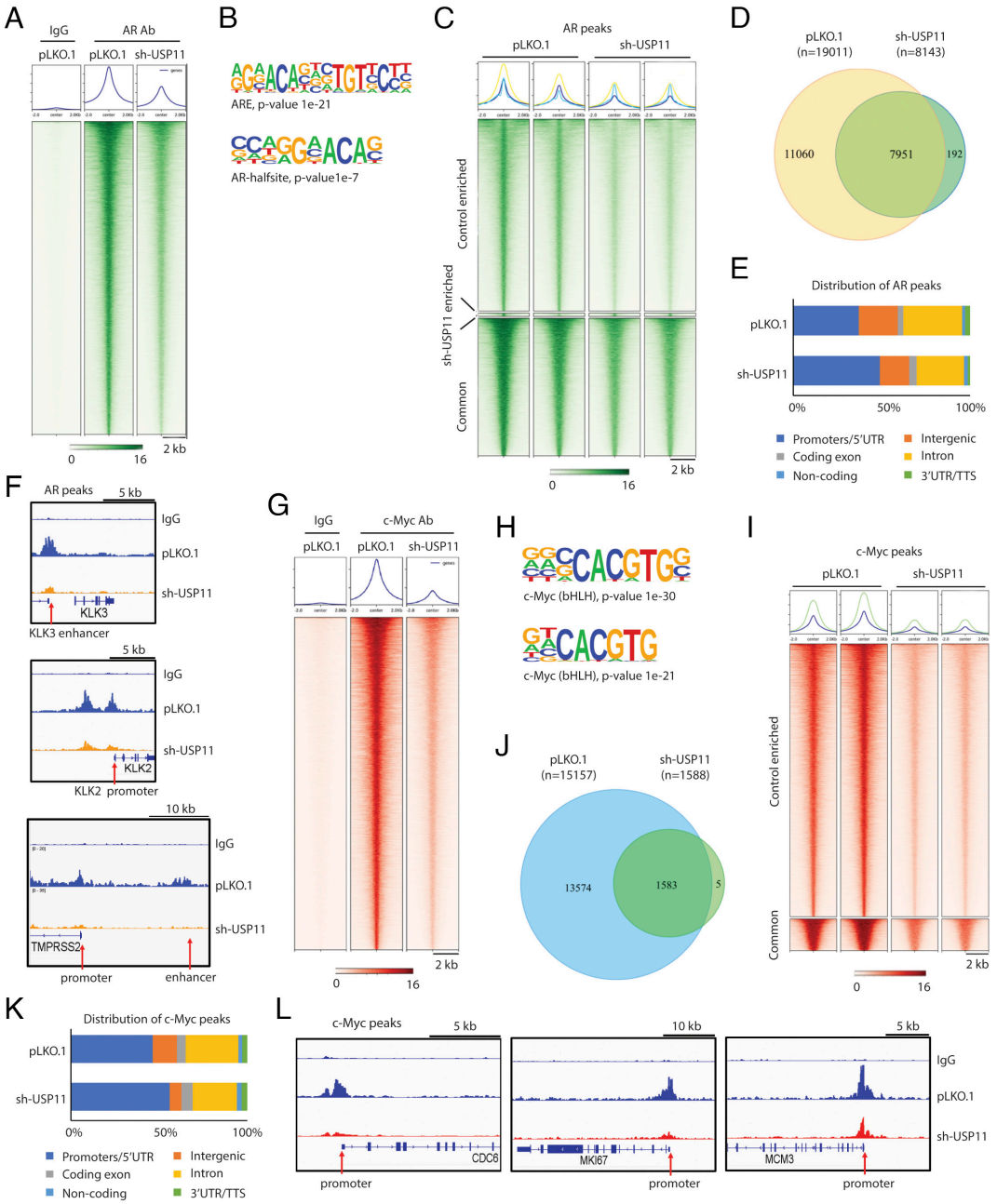

Fig. 3. (*A*) Heatmap showing AR ChIP-seq peaks. CUT&RUN ChIP-seq studies were conducted on Rv1 cells (pLKO.1 or USP11-KD) using an AR antibody, or on Rv1 cells (pLKO.1) using IgG control antibody. (*B*) Homer Motif Analysis showing enrichment of AREs and AR half-site motifs on AR peaks. (*C* and *D*) Heatmap (*C*) and Venn diagram (*D*) showing AR ChIP-seq peaks in control and USP11-KD Rv1 cells. (*E*) Genome distribution of AR peaks in control and USP11-KD Rv1 cells. (*F*) Signal track images showing AR peaks at the KLK3 enhancer, KLK2 promoter, and TMPRSS2 promoter/enhancer (indicated by arrows) in control and USP11-KD Rv1 cells. (*G*) Heatmap showing c-Myc ChIP-seq peaks. CUT&RUN ChIP-seq studies were conducted on Rv1 cells (pLKO.1 or USP11-KD) using c-Myc antibody or on Rv1 cells (pLKO.1) using IgG control antibody. (*H*) Homer Motif Analysis showing c-Myc binding motif enrichment on c-Myc peaks. (*I* and *J*) Heatmaps (*I*) and Venn diagram (*J*) showing c-Myc ChIP-seq peaks in control and USP11-KD Rv1 cells. (*K*) Genome distribution of c-Myc peaks in control and USP11-KD Rv1 cells. (*L*) Signal track images showing c-Myc peaks at CDC6, MKI67, and MCM3 promoters (indicated by arrows) in control and USP11-KD Rv1 cells.

KD also reduced the global c-Myc peaks (Fig. 3*G*). Among the c-Myc peaks, ~90% (13,574 of 15,157) showed a statistically significant reduction in size after USP11 KD, while ~10% (1,583 of 15,157) showed peak size reductions that were not significant (Fig. 3 *I* and *J*). c-Myc peak distribution across chromosomal locations was also notably changed by USP11 KD (Fig. 3*K*). As examples, USP11 KD decreased c-Myc peak signals on the promoters of CDC6, MKI67, MCM3 (Fig. 3*L*) and other c-Myc target genes (*SI Appendix*, Fig. S3*C*).

These findings overall indicate that USP11 plays a key role in promoting genome-wide binding of both AR and c-Myc.

USP11 Promotes Expression of AR and c-Myc mRNA by Deubiquitinating H2A-Ub on Their Promoters. Our RNA-seq and qRT-PCR analyses indicate that USP11 promotes expression of AR and c-Myc mRNAs (Fig. 2). USP11 is known to up-regulate gene expression by deubiquitinating monoubiquitinated histone H2A at lysine 119 (H2A-Ub), a repressive mark. To determine whether this activity underlies upregulation of AR and c-Myc mRNAs, we performed ChIP-PCR analysis of both USP11 and H2A-Ub (the latter using an antibody recognizing Ubiquityl-Histone H2A at K119) on the AR and c-Myc promoters in Rv1 cells and found that USP11 enriched on both, an enrichment that decreased after USP11 KD (Fig. 4 *A* and *B*). Interestingly, USP11 KD increased enrichment of H2A-Ub on the AR and c-Myc promoters (Fig. 4 *A* and *B*), suggesting overall that USP11 binds to and deubiquitinates H2A-Ub on both promoters, increasing transcription at both sites.

USP11 Deubiquitinates and Stabilizes AR and c-Myc Protein to Increase Their Levels. We next asked whether USP11 deubiquitinates AR and c-Myc proteins. To do so, we overexpressed wild-type HA-tagged USP11 in 293T cells transfected with Flag-tagged AR or Flag-tagged c-Myc and observed relatively increased protein (Fig. 4 *C* and *D*), but not mRNA (*SI Appendix*, Fig. S4 *A* and *B*), levels of Flag-AR and Flag-c-Myc in those cells. By contrast, overexpression of a catalytic-inactive USP11 mutant (CS) in the same cell contexts had no effect (Fig. 4 *C* and *D*), indicating that USP11 catalytic activity is required for observed increases in protein levels of Flag-AR or Flag-c-Myc.

To determine whether USP11 interacts with AR or c-Myc, we performed coimmunoprecipitation (Co-IP) analysis of endogenous USP11, AR, or c-Myc proteins in Rv1 cells. IP with a USP11 antibody followed by AR immunoblot (Fig. 4 *E*, *Left* panel) or IP with an AR antibody followed by USP11 immunoblot (Fig. 4 *E*, *Right* panel) revealed AR/USP11 coprecipitation. In comparable analysis, c-Myc and USP11 were also coprecipitated in Rv1 cells (Fig. 4*F*).

Next, to map domains critical for these interactions, we transfected 293T cells with constructs encoding AR or USP11 truncation mutants and performed Co-IP analysis. We found that HA-USP11 coprecipitated with the Flag-tagged AR ligand-binding domain (LBD) but not its N-terminal transactivation domain (N-TAD) or DNA-binding domain (DBD) (Fig. 4*G*). HA-AR coprecipitated with the Flag-tagged USP11 N-terminal fragment (N) but not with its C-terminal fragment (C) (Fig. 4*H*, and *SI Appendix*, Fig. S4C). These analyses indicate that the AR LBD interacts with the USP11 N terminus (*SI Appendix*, Fig. S4*D*). In comparable analysis, HA-USP11 coprecipitated with Flag-tagged c-Myc mutant lacking the N terminus (ΔN) but did not interact with a c-Myc ΔC mutant (Fig. 4*I*). HA-c-Myc coprecipitated with the USP11 C-terminal fragment (C) (Fig. 4*J*). Finally, when we divided the USP11 C-terminal fragment into catalytic domain 1, UBL2, and catalytic domain 2 (*SI Appendix*, Fig. S4*C*), we observed HA-c-Myc coprecipitation with the UBL2 and catalytic domain 2 (Fig. 4*J*). These analyses indicate that the c-Myc C terminus interacts with both the UBL2 and catalytic domain 2 of USP11 (*SI Appendix*, Fig. S4*E*). Finally, we used the mapped domains of USP11, AR, and c-Myc as input in Alphafold2 to predict the 3D interaction model. Helices 6 and 7 of the AR LBD are predicted to interact with the interface formed by DUSP and UBL domains of USP11 (*SI Appendix*, Fig. S4 *F* and *G*). The basic-helix1-loop of c-Myc C terminus is predicted to interact with the interface formed by UBL2 and catalytic domain 2 of USP11 (*SI Appendix*, Fig. S4 *H* and *I*).

Next, to determine whether USP11 deubiquitinates AR, we coexpressed Flag-AR, Myc-tagged USP11, and/or HA-ubiquitin in 293T cells, lysed cells under denaturing condition, immunoprecipitated Flag-AR with anti-Flag M2 beads and performed western blotting with HA antibodies to monitor Flag-AR polyubiquitination. Overexpression of Myc-tagged USP11 with Flag-AR plus HA-ubiquitin decreased polyubiquitination of Flag-AR (Fig. 4*K*, lane 3) relative to cells overexpressing Flag-AR and HA-ubiquitin only (Fig. 4*K*, lane 2). Similarly, USP11 overexpression decreased polyubiquitination of Flag-c-Myc (Fig. 4*L*). To assess effects on endogenous AR, we knocked down USP11 in Rv1 cells, lysed cells under denaturing condition, and immunoprecipitated AR with AR antibodies, followed by western blotting with ubiquitin antibodies. USP11 KD increased AR ubiquitination in Rv1 cells (Fig. 4*M*, lane 4 vs. lane 3). Similarly, USP11 KD increased c-Myc ubiquitination in Rv1 cells (Fig. 4*N*, lane 4 vs. lane 3).

To determine whether USP11 alters AR or c-Myc stability, we performed cycloheximide chase experiments to determine the half-life of endogenous AR or c-Myc in Rv1 cells after USP11 overexpression or KD. USP11 overexpression increased AR half-life from ~4 h (control) to 8 h (Fig. 4 *O* and *P*), whereas USP11 KD decreased AR half-life from ~4 h (control) to 2.5 h (*SI Appendix*, Fig. S4 *J* and *K*). In comparable analysis, USP11 overexpression increased c-Myc half-life from ~15 min (control) to 45 min (Fig. 4 *Q* and *R*). The short half-life of c-Myc (~15 min) did not allow us to assess whether USP11 KD would reduce the c-Myc half-life.

Overall, these results support the idea that both AR and c-Myc are USP11 substrates and that their deubiquitination by USP11 increases their stability and protein levels.

USP11 May Promote the Chromatin Binding of AR and c-Myc through H2A Deubiquitination. USP11 catalyzes H2A deubiquitination, and H2A-Ub represses gene expression (24, 25). Given its interaction with AR and c-Myc (Fig. 4 *E–J*), we asked whether USP11 regulates chromatin binding of AR and c-Myc via H2A deubiquitination. To confirm that USP11 catalyzes H2A deubiquitination, we overexpressed or knocked down USP11 in Rv1 cells followed by western blot analysis of H2A-Ub. Overexpression of wild-type USP11 decreased the level of H2A-Ub, whereas overexpression of USP11 catalytic-inactive mutant had no effect (*SI Appendix*, Fig. S5*A*), supporting a role of USP11 in H2A deubiquitination. USP11 KD had no apparent effect on the level of H2A-Ub (*SI Appendix*, Fig. S5*B*), suggesting that USP11 may catalyze H2A deubiquitination on select chromatin sites. ChIP-PCR of USP11 in Rv1 cells indicated USP11 enrichment on AR target genes such as the KLK3 enhancer, KLK2 promoter, or NKX3-1 promoter, and these effects were attenuated by USP11 KD (*SI Appendix*, Fig. S5*C*). ChIP-PCR of H2A-Ub and AR indicated that USP11 KD increased H2A-Ub levels and decreased AR levels on these target genes (*SI Appendix*, Fig. S5 *D* and *E*). Similarly, USP11 also showed enrichment on promoter regions of the c-Myc target genes CCNE2, CDK4, E2F2, and TERT

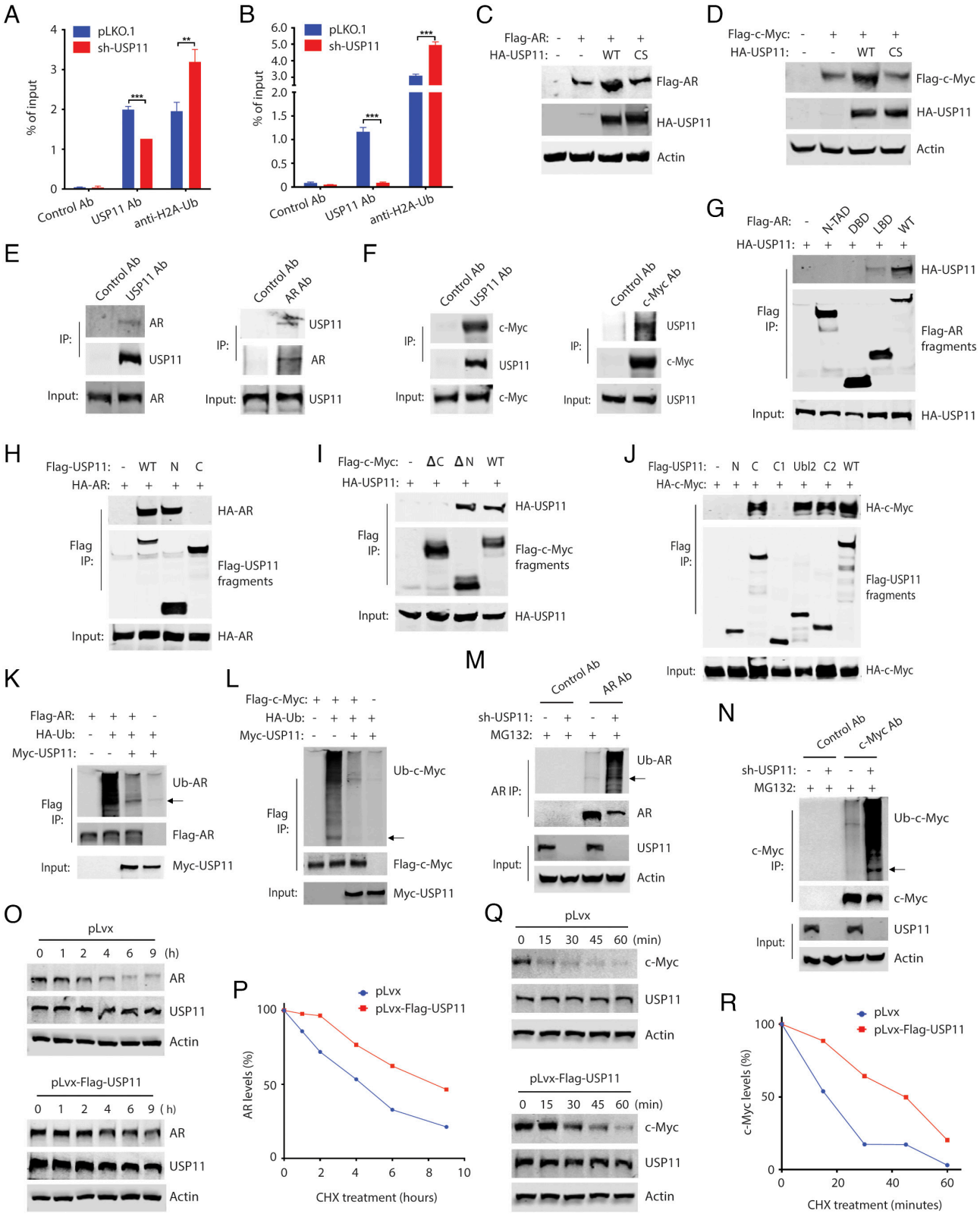

Fig. 4. (*A* and *B*) ChIP-PCR of USP11 or H2A-Ub on AR (*A*) or c-Myc (*B*) promoters in Rv1 cells (control or USP11-KD). ChIP assays were performed with control, USP11, or H2A-Ub antibodies. Precipitated chromatin was analyzed by qPCR for AR or c-Myc promoter regions. (*C* and *D*) Transfection of HA-USP11-WT, but not HA-USP11-CS, increases levels of coexpressed Flag-AR (*C*) or Flag-c-Myc (*D*) in 293T cells. (*E*) Co-IP of AR with USP11 (*Left* panel) or Co-IP of USP11 with AR (*Right* panel) in Rv1 cells. (*F*) Co-IP of c-Myc with USP11 (*Left* panel) or co-IP of USP11 with c-Myc (*Right* panel) in Rv1 cells. (*G*) USP11 interaction with the AR LBD. (*H*) AR interaction with the USP11 N-terminal fragment. (*I*) USP11 interaction with the c-Myc C-terminal transaction domain. (*J*) c-Myc interaction with the USP11 Ubl2 or catalytic domain 2. (*K* and *L*) Overexpression of myc-tagged USP11 decreases ubiquitination of Flag-AR (*K*) or Flag-c-Myc (*L*). Arrows indicate the position Flag-AR or Flag-c-Myc. (*M* and *N*) USP11 KD in Rv1 cells increases ubiquitination of AR (*M*) or c-Myc (*N*). Arrows indicate the position of AR or c-Myc. (*O* and *P*) USP11 overexpression in Rv1 cells increases AR half-life. Cells were treated with cycloheximide (CHX, 50 μg/mL). Lysates were collected at indicated times and analyzed by western blotting (*O*). AR half-life was quantified (*P*). (*Q* and *R*) USP11 overexpression in Rv1 cells increases c-Myc half-life. Experimental procedures are as described in *O* and *P*.

(*SI Appendix*, Fig. S5*F*), and USP11 KD increased H2A-Ub levels and decreased c-Myc levels on these targets (*SI Appendix*, Fig. S5 *G* and *H*). These results overall suggest that USP11 may facilitate binding of AR and c-Myc to their respective target genes in part through H2A deubiquitination. To further evaluate this possibility, we isolated chromatin from cells and analyzed the chromatin-bound level of AR or c-Myc. In the whole cell lysate (WCL), we forced to reexpress AR or c-Myc in USP11-KD Rv1 cells and restore their levels to those seen in control cells (*SI Appendix*, Fig. S5 *I* and *J*, *Left* panel). In contrast, reexpression of AR or c-Myc only partly restored their levels in the chromatin fraction of USP11-KD cells (*SI Appendix*, Fig. S5 *I* and *J*, *Right* panel). These results suggest that USP11 may have an additional role in promoting the chromatin binding of AR and c-Myc.

USP11 Catalytic Activity Is Required for Its Regulation of AR and c-Myc. To confirm that USP11 catalytic activity is required for the effects described above, we silenced USP11 expression in Rv1 cells and then reexpressed HA-tagged wild-type or catalytic-inactive forms of USP11 to levels seen in control cells (*SI Appendix*, Fig. S5*K*). Of note, we introduced silent mutations at the shRNA targeting site of mis-expressed USP11 constructs that could not be silenced by USP11 shRNA. USP11 KD significantly reduced AR and c-Myc protein levels in Rv1 cells (*SI Appendix*, Fig. S5*K*). Reexpression of wild-type USP11 in USP11-KD cells (designated $USP11^{WT}$ cells) fully restored AR and c-Myc levels, whereas reexpression of the corresponding catalytic-inactive mutant of USP11 in USP11-KD cells (designated $USP11^{CS}$ cells) only slightly increased AR and c-Myc protein levels (*SI Appendix*, Fig. S5*K*). These results indicate that USP11 catalytic activity is required to maintain AR and c-Myc levels in Rv1 cells.

Next, we performed ChIP-PCR using anti-HA antibodies, to detect HA-tagged USP11, or H2A-Ub antibodies in $USP11^{WT}$ and $USP11^{CS}$ cells. As expected, ChIP-PCR with HA antibodies revealed enrichment of wild-type USP11 on the promoters of AR (*SI Appendix*, Fig. S5*L*) and c-Myc (*SI Appendix*, Fig. S5*M*) genes and on the AR (*SI Appendix*, Fig. S5*N*) and c-Myc (*SI Appendix*, Fig. S5*O*) target genes named above. Surprisingly, we observed significantly reduced levels of the USP11 CS mutant on chromatin loci tested (*SI Appendix*, Fig. S5 *L–O*). Relative to $USP11^{WT}$ cells, $USP11^{CS}$ cells showed increased H2A-Ub levels on the AR (*SI Appendix*, Fig. S5*L*) and c-Myc (*SI Appendix*, Fig. S5*M*) promoters and on AR (*SI Appendix*, Fig. S5*P*) and c-Myc (*SI Appendix*, Fig. S5*Q*) target genes.

Together, these results suggest that USP11 catalytic activity is required to remove H2A-Ub marks on regulatory elements of AR, c-Myc, or their target genes.

USP11 Catalytic Activity Regulates Genome-Wide Binding of AR and c-Myc. To evaluate whether USP11 catalytic activity impacts global chromatin binding by AR and c-Myc, we performed ChIP-seq analysis of $USP11^{WT}$ and $USP11^{CS}$ cells (described in *SI Appendix*, Fig. S5*K*) using HA, AR, or c-Myc antibodies (23). We note that currently available anti-USP11 antibodies are not suitable for ChIP-seq analysis, and thus we performed ChIP-seq of ectopic HA-USP11 using the HA antibody as an alternative means to assess USP11 global chromatin binding. In $USP11^{WT}$ cells, we detected 52,075 HA-USP11-WT peaks by ChIP-seq using HA versus control antibody (Fig. 5*A*). As another control, no peaks were detected in the HA ChIP-seq performed on Rv1 cells (Fig. 5*A*). Homer motif analysis of HA-USP11-WT peaks revealed enrichment of AR half-sites and c-Myc binding motifs (Fig. 5*B* and *SI Appendix*, Table S2), consistent with our finding that USP11 may interact with AR and c-Myc on chromatin (*SI Appendix*, Fig. S5).

By contrast, $USP11^{CS}$ cells showed a global reduction in chromatin binding by HA-USP11-CS relative to WT HA-USP11 (Fig. 5*A*), consistent with our ChIP-PCR analysis showing that USP11 catalytic activity is required for target binding (*SI Appendix*, Fig. S5 *L–O*). We also observed HA-USP11-WT peaks at AR or c-Myc gene promoter regions where we had detected no HA-USP11-CS peaks (Fig. 5 *C* and *D*), consistent with our ChIP-PCR data showing that USP11 binds to AR and c-Myc promoters to induce H2A deubiquitination (Fig. 4 *A* and *B* and *SI Appendix*, Fig. S5 *L* and *M*). Relative to $USP11^{WT}$ cells, $USP11^{CS}$ cells showed a global reduction in AR peaks, among which ~72% (9,299 of 12,905) showed a statistically significant reduction in peak size, while ~28% (3,606 of 12,905) showed detectable reductions that were not statistically significant (Fig. 5 *E* and *F* and *SI Appendix*, Fig. S6*A*). The distribution of AR peaks across distinct chromosomal locations also differed in $USP11^{WT}$ versus $USP11^{CS}$ cells (Fig. 5*G*). For example, compared with $USP11^{WT}$ cells, $USP11^{CS}$ cells showed the reduced AR peak signals on the KLK3 enhancer or NKX3-1 promoter (Fig. 5*H*). ~49% (6,164 of 12,496) of AR peaks overlapped with HA-USP11-WT peaks (Fig. 5*I*), suggesting the interaction between USP11 and AR on select AR target genes. Furthermore, we compared the reduced AR peaks after USP11-KD (i.e., USP11-dependent AR peaks, Fig. 3*D*) and the reduced AR peaks in $USP11^{CS}$ cells (i.e., USP11 catalytic-dependent AR peaks, Fig. 5*F*). ~50% (9,294/18,756) of USP11-dependent AR peaks overlap with catalytic-dependent AR peaks (*SI Appendix*, Fig. S6*B*), indicating that these AR peaks (50%) require the USP11 catalytic activity. These results also suggest that USP11 may regulate other AR peaks (50%) independent of its catalytic activity.

Compared with $USP11^{WT}$ cells, $USP11^{CS}$ cells showed a global reduction of c-Myc peaks, among which ~39% (4,502 of 11,556) showed a statistically significant reduction in peak size, while ~65% (7,504 of 11,556) showed detectable reductions in peak size that were not statistically significant (Fig. 5 *J* and *K* and *SI Appendix*, Fig. S6*C*). Likewise, distribution of c-Myc peaks across distinct chromosomal locations was altered in $USP11^{WT}$ relative to $USP11^{CS}$ cells (Fig. 5*L*). As example, compared with $USP11^{WT}$ cells, $USP11^{CS}$ cells showed the reduced c-Myc peak signals on CDK4 and LDHA promoters (Fig. 5*M*). ~73% (8,305 of 11,316) of c-Myc peaks overlapped with HA-USP11-WT peaks (Fig. 5*N*), suggesting the interaction between USP11 and c-Myc on select c-Myc target genes. Finally, we compared the reduced c-Myc peaks after USP11-KD (i.e., USP11-dependent c-Myc peaks, Fig. 3*J*) and the reduced c-Myc peaks in $USP11^{CS}$ cells (i.e., USP11 catalytic-dependent c-Myc peaks, Fig. 5*K*). ~67% (9,630/14,333) of USP11-dependent c-Myc peaks overlap with catalytic-dependent c-Myc peaks (*SI Appendix*, Fig. S6*D*), indicating that these c-Myc peaks (67%) require the USP11 catalytic activity. These results also suggest that USP11 may regulate some c-Myc peaks (33%) independent of its catalytic activity.

Together, these results indicate that USP11 catalytic activity regulates genome-wide binding of AR and c-Myc.

USP11 Promotes PCa Progression in Part through AR and c-Myc. Our results show that USP11 KD decreases AR and c-Myc levels and inhibits PCa cell growth (Fig. 1 *G–M*). To determine whether USP11 loss inhibits PCa cell growth via effects on AR and/or c-Myc, we reexpressed AR, c-Myc, or both in USP11-KD VCaP cells to levels seen in control cells (Fig. 6*A*). Reexpression of AR or c-Myc partly rescued defects in both colony formation (Fig. 6 *B* and *C*) and xenograft tumor growth (Fig. 6 *D* and *E*). Moreover, reexpression of both AR and c-Myc further rescued VCaP cell growth to an extent greater than expression of either gene alone

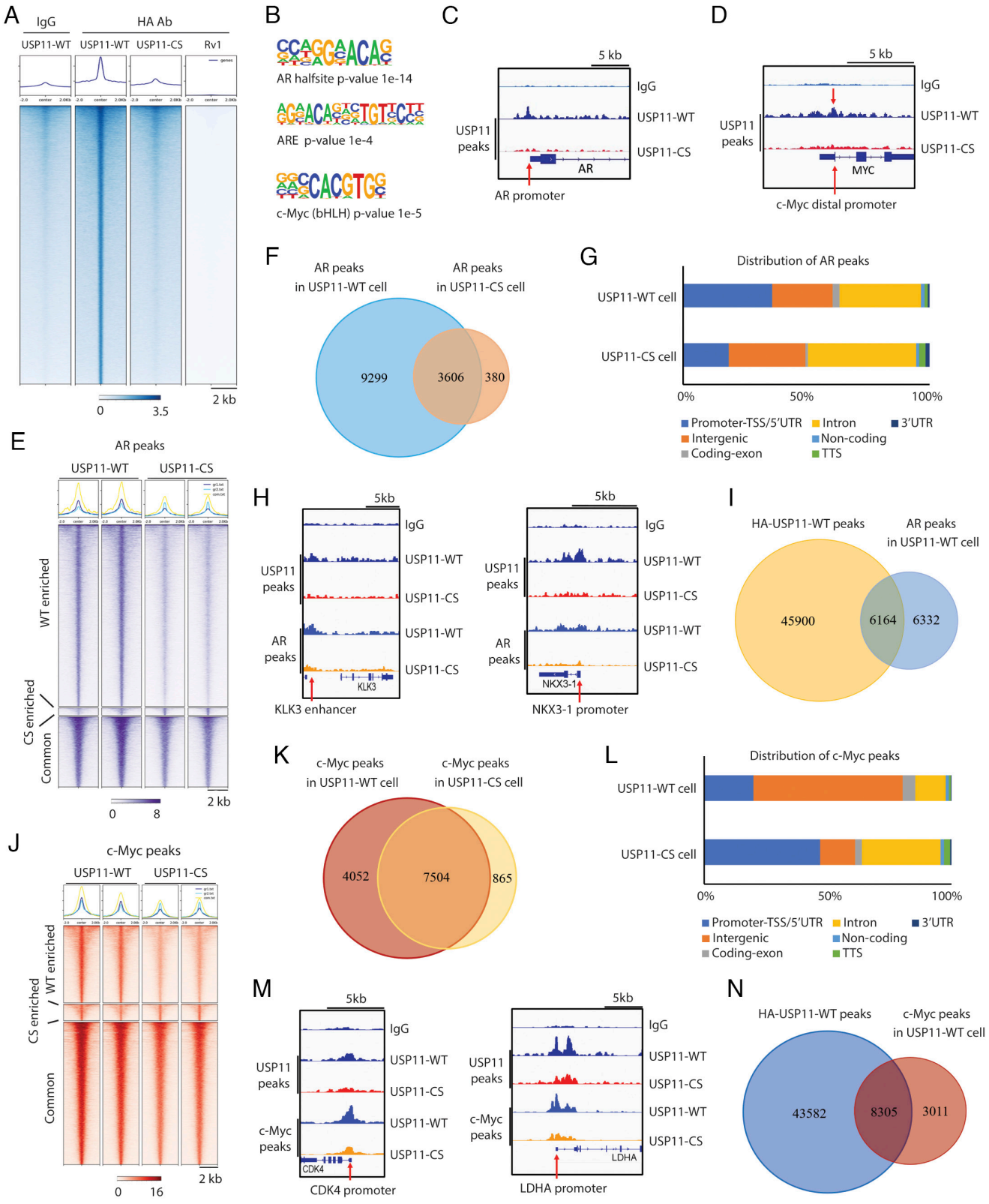

Fig. 5. (*A*) Heatmaps showing the chromatin binding by HA-USP11-WT and HA-USP11-CS. CUT&RUN ChIP-seq studies were conducted on the indicated cells using HA antibody, or on USP11^{WT} cells using IgG control antibody. (*B*) Homer motif analysis showing enrichment of AR half-site, ARE and c-Myc binding motifs on HA-USP11-WT peaks. (*C* and *D*) Signal track images showing the enrichment of HA-USP11-WT peaks, but not HA-USP11-CS peaks, at the AR (*C*) or c-Myc (*D*) promoters (indicated by arrow). (*E* and *F*) Heatmap (*E*) and Venn diagram (*F*) showing AR ChIP-seq peaks in USP11^{WT} and USP11^{CS} cells. (*G*) Genome distribution of AR peaks in USP11^{WT} and USP11^{CS} cells. (*H*) Signal track images showing HA-USP11 peaks and AR peaks at the KLK3 enhancer and NKX3-1 promoter (indicated by an arrow) in USP11^{WT} and USP11^{CS} cells. (*I*) Venn diagram showing overlap of HA-USP11-WT peaks with AR peaks in USP11^{WT} cells. (*J* and *K*) Heatmap (*J*) and Venn diagram (*K*) showing c-Myc ChIP-seq peaks in USP11^{WT} and USP11^{CS} cells. (*L*) Genome distribution of c-Myc peaks in USP11^{WT} and USP11^{CS} cells. (*M*) Signal track Images showing HA-USP11 peaks and c-Myc peaks at promoters (indicated by arrow) of indicated c-Myc target genes in USP11^{WT} and USP11^{CS} cells. (*N*) Venn diagram showing overlap of HA-USP11-WT peaks with c-Myc peaks in USP11^{WT} cells.

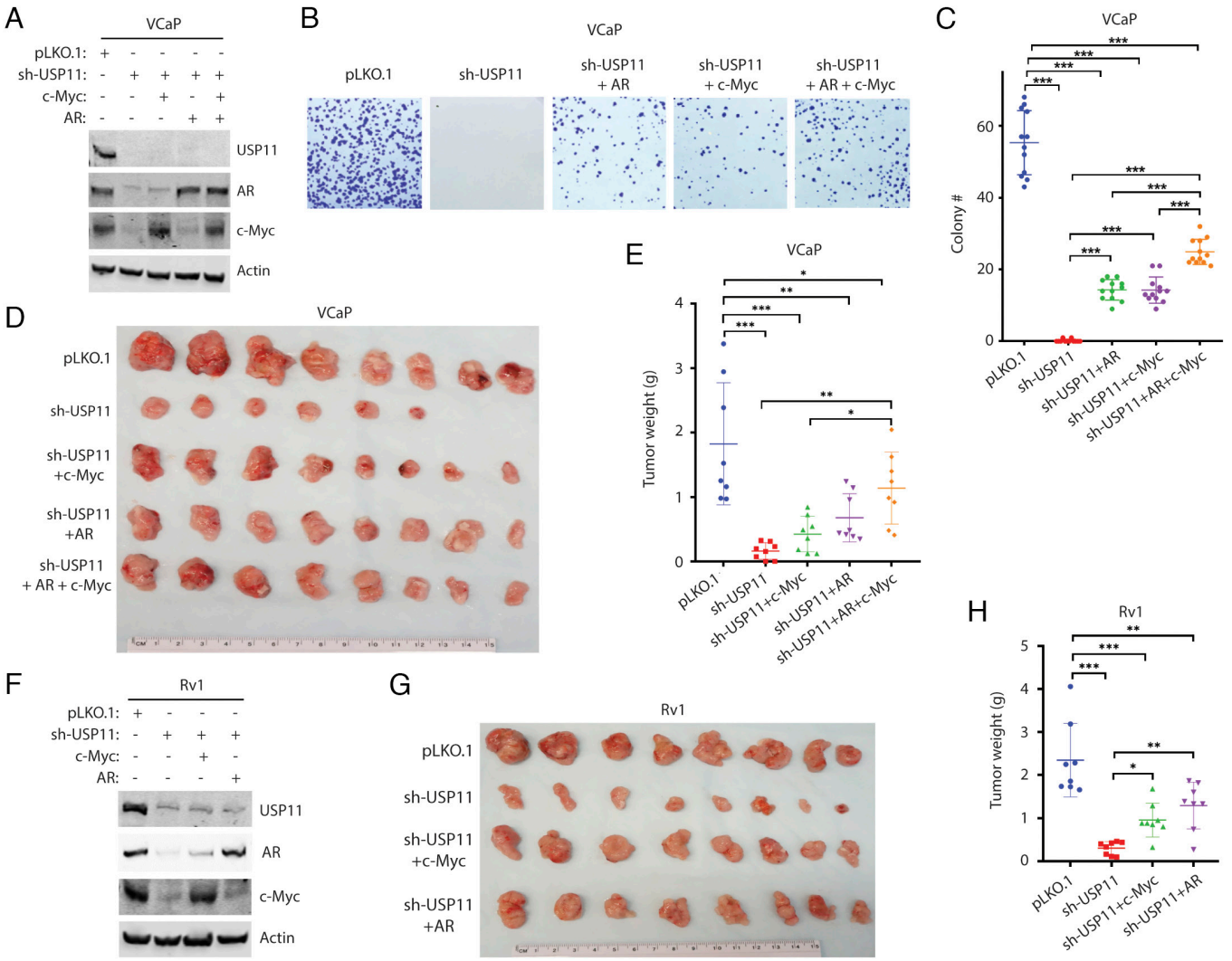

Fig. 6. (*A*) Western blots showing reexpression of AR, c-Myc, or both in USP11-KD VCaP cells. (*B* and *C*) Representative images (*B*) and quantification (*C*) of colony formation by USP11-KD VCaP cells reexpressing AR, c-Myc, or both. (*D* and *E*) AR and c-Myc reexpression in USP11-KD VCaP cells partly rescues xenograft tumor growth. Indicated VCaP cells were subcutaneously injected into athymic nude mice, xenograft tumors were collected 5 wk later (*D*), and tumor weight was quantified (*E*). (*F*) Western blots showing reexpression of AR or c-Myc in USP11-KD Rv1 cells. (*G* and *H*) AR or c-Myc reexpression in USP11-KD Rv1 cells partly rescues xenograft tumor growth. Indicated Rv1 cells were subcutaneously injected into athymic nude mice, xenograft tumors were collected 5 wk later (*G*), and tumor weight was quantified (*H*).

(Fig. 6 *B*–*E*). We also reexpressed AR or c-Myc in USP11-KD Rv1 cells (Fig. 6*F*) and observed partial rescue of colony formation (*SI Appendix*, Fig. S7 *A* and *B*) and xenograft tumor growth (Fig. 6 *G* and *H*). Similar to VCaP cells, reexpression of both AR and c-Myc further rescued the colony formation by USP11-KD Rv1 cells than expression of either gene alone (*SI Appendix*, Fig. S7*C*). In AR-negative DU145 cells, c-Myc reexpression in USP11-KD cells also partly rescued defects in colony formation (*SI Appendix*, Fig. S7 *D*–*F*). Overall, these results indicate that AR and/or c-Myc are key downstream effectors of USP11 in PCa cells.

USP11 Can be Targeted to Inhibit AR and c-Myc Activities in PCa Cells. Mitoxantrone (MTX) is a synthetic anthracenedione that intercalates into DNA and indues DNA damage, and it is also reportedly a USP11 catalytic inhibitor (26–28). We found that MTX treatment of Rv1 or VCaP cells decreased AR and c-Myc protein levels (*SI Appendix*, Fig. S8*A*). AR-V7 is a splicing variant of AR that lacks LBD, the domain that interacts with USP11 (Fig. 4*G*). MTX treatment had no effect on the level of AR-V7 (*SI Appendix*, Fig. S8*A*) likely because USP11 cannot interact with AR-V7. MTX treatment also decreased transcript levels of both AR (*SI Appendix*, Fig. S8 *B* and *C*) and c-Myc (*SI Appendix*, Fig. S8 *D* and *E*) target genes.

MTX treatment significantly inhibited colony formation by various PCa cells (*SI Appendix*, Fig. S8 *F*–*J*), effects that might be due to either MTX-induced DNA damage or to USP11 inhibition. To address this question, we overexpressed USP11-WT, USP11-CS, or a control construct in Rv1 or VCaP cells and then performed colony formation assays in the presence of either vehicle or MTX. For the vehicle-treated cells, overexpression of USP11-WT slightly increased colony formation (~1.5-fold) compared with control cells (*SI Appendix*, Fig. S8 *K* and *L*). In contrast, for MTX-treated cells, overexpression of USP11-WT highly increased colony formation (~5-fold for Rv1 and ~7-fold for VCaP) compared with control cells (*SI Appendix*, Fig. S8 *K* and *L*). Overexpression of USP11-CS had no effect on colony formation under either condition (*SI Appendix*, Fig. S8 *K* and *L*). These results indicate that overexpression of USP11-WT confers resistance to MTX in a manner dependent on its catalytic activity. These results also support that MTX inhibition of cell growth is mediated in part via USP11 catalytic inhibition.

Discussion

In this study, we find that USP11 promotes PCa cell growth partly through upregulation of the transcription factors AR and c-Myc. Deubiquitinases have been previously reported to regulate either AR or c-Myc: USP12, USP14, and USP22 can deubiquitinate and stabilize AR (8, 10, 29), while USP16, USP17, and USP28 deubiquitinate and stabilize c-Myc (30–32). Here, we find that USP11 up-regulates AR and c-Myc levels through two mechanisms, including deubiquitination of AR and c-Myc proteins to increase their stability, and deubiquitination of H2A-Ub on AR and c-Myc promoters to enhance their transcription.

Our findings differ from a reported function of USP11 as a tumor suppressor in PCa (21), a conclusion based on findings that USP11 knockout up-regulates PTEN and inhibits oncogene-induced fibroblast transformation or tumorigenesis in a TRAMP prostate tumor model. Those findings suggest that USP11 effects on PTEN may inhibit tumor initiation at early stages of prostate tumorigenesis. PTEN is frequently mutated or deleted in primary PCa, and ~50% CRPCs show loss of PTEN expression (33). Thus, USP11 may target other substrates in the PTEN-deficient PCa. Our study reveals a tumor-promoting role of USP11 in various PCa cells, regardless of PTEN status. Of note, stage-dependent oncogenic or tumor suppressor functions have been reported for other factors, such as TGF-β, which is tumor-suppressive at early stages of various cancers but tumor-promoting at later stages (34).

Our ChIP-seq studies showed that either USP11 KD or expression of a catalytic-inactive mutant form of USP11 inhibits genome-wide binding of AR and c-Myc, supporting the idea that USP11 catalytic activity regulates those activities. Global reduction in AR and c-Myc chromatin binding upon USP11 inhibition may result from reduced AR and c-Myc levels, but we cannot exclude the possibility that USP11-mediated regulation of H2A-Ub may also contribute to the process. Future ChIP-seq studies of H2A-Ub will be needed to evaluate the role of H2A-Ub deubiquitination in USP11-dependent chromatin binding by AR and c-Myc.

Other questions remain from this study. First, does USP11 regulate other substrates in PCa cells? Reexpression of both AR and c-Myc cannot fully rescue the growth defect of USP11-KD PCa cells. Our RNA-seq study shows that USP11 regulates expression of other genes besides AR and c-Myc targets. Thus, it remains to be determined whether USP11 also regulates other transcription factor(s) to drive PCa progression. Second, does USP11 have catalytic-independent role in regulation of AR and c-Myc? Our study identified several catalytic-dependent mechanisms of USP11 in regulating levels and chromatin binding of AR and c-Myc. In addition, our results suggest a minor catalytic-independent function of USP11 in the process. Future work is needed to determine whether USP11-mediated protein–protein interaction may also regulate AR and c-Myc independent of its catalytic activity.

In summary, we reveal a tumor-promoting role for USP11 in aggressive PCa through upregulation of AR and c-Myc activities. Our study supports USP11 as a target for potential PCa therapy.

Materials and Methods

CUT&RUN ChIP Sequencing (ChIP-seq) Analysis. Rv1 cells were transduced with sh-control or sh-USP11 lentivirus for 48 h. Alternatively, USP11-KD Rv1 cells were transduced with HA-USP11-WT or HA-USP11-CS lentivirus for 48 h. Two biological replicates (5×10^5 living cells per replicate) were used for ChIP-seq preparation, following the CUT&RUN kit protocol (EpiCypher). CUT&RUN procedures were detailed previously (35), and data analysis is described in *SI Appendix, Supplemental Methods*.

Xenograft Tumor Models. Athymic nude mice were purchased from the Jackson Laboratory and housed in the animal facility at the University of Maryland School of Medicine. The animal studies were approved by the Institutional Animal Care and Use Committee (IACUC #0122010) and conducted following the University's animal policy in accordance with NIH guidelines. The experimental procedures were detailed previously (36). Eight-week-old male athymic nude mice (n = 8 per group) were subcutaneously injected with Rv1, C4-2, PC3 cells (1×10^6 cells) or VCaP cells (2×10^6 cells). Four to five weeks postinjection, xenograft tumors were collected, and tumor weights were measured using a digital balance.

IHC Staining of USP11 on PCa TMAs. Commercial PCa TMAs were purchased from the Molecular Pathology Core of Vancouver Prostate Centre at the University of British Columbia. PCa tissue collection for TMA preparation was approved by the UBC Clinical Research Ethics Board # H09-06128. All PCa tissue samples on the TMAs are unidentifiable and cannot be linked back to the patients. We and the provider have no access to the identification of PCa patients. 4-μm thick sections of PCa TMAs were used for IHC staining with USP11 antibody (ab109232; 1:100 dilution). Staining procedures were detailed previously (37, 38), and staining quantification is described in *SI Appendix, Supplemental Methods*.

Statistical Analysis. Experiments were performed independently three times in triplicate. Biological triplicates from one representative experiment were used for quantification and presented as means ± SD (n = 3). Statistical analysis was performed using GraphPad Prism software. Student's *t* test (two-tailed) was used to compare differences between two groups of datasets, while ANOVA was used to compare differences among more than two groups of datasets. Kruskal–Wallis test was used to compare differences of USP11 H-score among various PCa groups. For all statistical analyses, differences were labeled as follows: ns, not significant; $*P < 0.05$; $**P < 0.01$; $***P < 0.001$. *P*-values < 0.05 were considered statistically significant.

Data, Materials, and Software Availability. Raw data related to RNA-seq (GSE268124) and CUT&RUN ChIP-seq (GSE268252) have been deposited in the GEO database (22, 23).

ACKNOWLEDGMENTS. This work was supported by National Cancer Institute Grant R01CA244667 and Department of Defense Grant PC210437 (to J.Q.). This research was partly supported by funds through the Maryland Department of Health's Cigarette Restitution Fund Program (CH-649-CRF) and the National Cancer Institute–Cancer Center Support Grant–P30CA134274. Part of A.H.'s time was supported by a Merit Review Award (I01 BX000545), Medical Research Service, U.S. Department of Veterans Affairs, and a Baltimore Veterans Affairs Medical Center VALOR Precision Oncology Pilot Award (ID #21PILO02), Prostate Cancer Foundation. Part of Z.Z.'s time was supported by National Institute of General Medical Sciences Grant R01GM129468. Part of H.Z.O.'s time was supported by Terry Fox New Frontiers Program Project Grant for supporting Vancouver Prostate Centre members.

1. P. A. Watson, V. K. Arora, C. L. Sawyers, Emerging mechanisms of resistance to androgen receptor inhibitors in prostate cancer. *Nat. Rev. Cancer* **15**, 701–711 (2015).
2. K. T. Schmidt, A. D. R. Huitema, C. H. Chau, W. D. Figg, Resistance to second-generation androgen receptor antagonists in prostate cancer. *Nat. Rev. Urol.* **18**, 209–226 (2021).
3. B. Gurel *et al.*, Nuclear MYC protein overexpression is an early alteration in human prostate carcinogenesis. *Mod. Pathol.* **21**, 1156–1167 (2008).
4. K. Ellwood-Yen *et al.*, Myc-driven murine prostate cancer shares molecular features with human prostate tumors. *Cancer Cell* **4**, 223–238 (2003).
5. S. Bai *et al.*, A positive role of c-Myc in regulating androgen receptor and its splice variants in prostate cancer. *Oncogene* **38**, 4977–4989 (2019).
6. M. J. Wu *et al.*, Targeting KDM4B that coactivates c-Myc-regulated metabolism to suppress tumor growth in castration-resistant prostate cancer. *Theranostics* **11**, 7779–7796 (2021).
7. J. Monga, D. Subramani, A. Bharathan, J. Ghosh, Pharmacological and genetic targeting of 5-lipoxygenase interrupts c-Myc oncogenic signaling and kills enzalutamide-resistant prostate cancer cells via apoptosis. *Sci. Rep.* **10**, 6649 (2020).
8. R. S. Schrecengost *et al.*, USP22 regulates oncogenic signaling pathways to drive lethal cancer progression. *Cancer Res.* **74**, 272–286 (2014).
9. S. T. Chen *et al.*, The deubiquitinating enzyme USP7 regulates androgen receptor activity by modulating its binding to chromatin. *J. Biol. Chem.* **290**, 21713–21723 (2015).
10. U. L. Burska *et al.*, Deubiquitinating enzyme Usp12 is a novel co-activator of the androgen receptor. *J. Biol. Chem.* **288**, 32641–32650 (2013).

11. Y. Chen, X. X. Sun, R. C. Sears, M. S. Dai, Writing and erasing MYC ubiquitination and SUMOylation. *Genes Dis.* **6**, 359–371 (2019).
12. Y. Liao, D. Zhou, P. Wang, M. Yang, N. Jiang, Ubiquitin specific peptidase 11 as a novel therapeutic target for cancer management. *Cell Death Discov.* **8**, 292 (2022).
13. G. N. Maertens, S. El Messaoudi-Aubert, S. Elderkin, K. Hiom, G. Peters, Ubiquitin-specific proteases 7 and 11 modulate Polycomb regulation of the INK4a tumour suppressor. *EMBO J.* **29**, 2553–2565 (2010).
14. B. Kapadia *et al.*, Fatty acid synthase induced S6Kinase facilitates USP11-eIF4B complex formation for sustained oncogenic translation in DLBCL. *Nat. Commun.* **9**, 829 (2018).
15. Z. Zhou *et al.*, Regulation of XIAP turnover reveals a role for USP11 in promotion of tumorigenesis. *EBioMedicine* **15**, 48–61 (2017).
16. H. Sun *et al.*, USP11 promotes growth and metastasis of colorectal cancer via PPP1CA-mediated activation of ERK/MAPK signaling pathway. *EBioMedicine* **48**, 236–247 (2019).
17. H. C. Wu *et al.*, USP11 regulates PML stability to control Notch-induced malignancy in brain tumours. *Nat. Commun.* **5**, 3214 (2014).
18. T. Deng *et al.*, Deubiquitylation and stabilization of p21 by USP11 is critical for cell-cycle progression and DNA damage responses. *Proc. Natl. Acad. Sci. U.S.A.* **115**, 4678–4683 (2018).
19. L. Qiao *et al.*, The E2F1/USP11 positive feedback loop promotes hepatocellular carcinoma metastasis and inhibits autophagy by activating ERK/mTOR pathway. *Cancer Lett.* **514**, 63–78 (2021).
20. W. Wang, J. Wang, H. Yan, K. Zhang, Y. Liu, Upregulation of USP11 promotes epithelial-to-mesenchymal transition by deubiquitinating snail in ovarian cancer. *Oncol. Rep.* **41**, 1739–1748 (2019).
21. M. K. Park *et al.*, PTEN self-regulates through USP11 via the PI3K-FOXO pathway to stabilize tumor suppression. *Nat. Commun.* **10**, 636 (2019).
22. J. Qi, M. Pornour, USP11 promotes prostate cancer progression by upregulating AR and c-Myc activity [RNA-seq]. Gene Expression Omnibus. https://www.ncbi.nlm.nih.gov/geo/query/acc.cgi?acc=GSE268124. Deposited 22 May 2024.
23. J. Qi, M. Pornour, USP11 promotes prostate cancer progression by upregulating AR and c-Myc activity [CUT&RUN]. Gene Expression Omnibus. https://www.ncbi.nlm.nih.gov/geo/query/acc.cgi?acc=GSE268252. Deposited 23 May 2024.
24. X. Ting *et al.*, USP11 acts as a histone deubiquitinase functioning in chromatin reorganization during DNA repair. *Nucleic Acids Res.* **47**, 9721–9740 (2019).
25. S. Tamburri *et al.*, Histone H2AK119 mono-ubiquitination is essential for polycomb-mediated transcriptional repression. *Mol. Cell* **77**, 840–856.e845 (2020).
26. R. A. Burkhart *et al.*, Mitoxantrone targets human ubiquitin-specific peptidase 11 (USP11) and is a potent inhibitor of pancreatic cancer cell survival. *Mol. Cancer Res.* **11**, 901–911 (2013).
27. I. F. Tannock *et al.*, Chemotherapy with mitoxantrone plus prednisone or prednisone alone for symptomatic hormone-resistant prostate cancer: A Canadian randomized trial with palliative end points. *J. Clin. Oncol.* **14**, 1756–1764 (1996).
28. B. A. Teply, R. J. Hauke, Chemotherapy options in castration-resistant prostate cancer. *Indian J. Urol.* **32**, 262–270 (2016).
29. Y. Liao *et al.*, Proteasome-associated deubiquitinase ubiquitin-specific protease 14 regulates prostate cancer proliferation by deubiquitinating and stabilizing androgen receptor. *Cell Death Dis.* **8**, e2585 (2017).
30. J. Ge *et al.*, USP16 regulates castration-resistant prostate cancer cell proliferation by deubiquitinating and stablizing c-Myc. *J. Exp. Clin. Cancer Res.* **40**, 59 (2021).
31. M. Nagasaka *et al.*, The deubiquitinating enzyme USP17 regulates c-Myc levels and controls cell proliferation and glycolysis. *FEBS Lett.* **596**, 465–478 (2022).
32. N. Popov *et al.*, The ubiquitin-specific protease USP28 is required for MYC stability. *Nat. Cell Biol.* **9**, 765–774 (2007).
33. R. Ferraldeschi *et al.*, PTEN protein loss and clinical outcome from castration-resistant prostate cancer treated with abiraterone acetate. *Eur. Urol.* **67**, 795–802 (2015).
34. R. Derynck, R. J. Akhurst, A. Balmain, TGF-beta signaling in tumor suppression and cancer progression. *Nat. Genet.* **29**, 117–129 (2001).
35. H. Y. Jeon *et al.*, SMAD3 promotes expression and activity of the androgen receptor in prostate cancer. *Nucleic Acids Res.* **51**, 2655–2670 (2023).
36. S. Xu *et al.*, p300-mediated acetylation of histone demethylase JMJD1A prevents its degradation by ubiquitin ligase STUB1 and enhances its activity in prostate cancer. *Cancer Res.* **80**, 3074–3087 (2020).
37. L. Fan *et al.*, Regulation of c-Myc expression by the histone demethylase JMJD1A is essential for prostate cancer cell growth and survival. *Oncogene* **35**, 2441–2452 (2016).
38. L. Fan *et al.*, Histone demethylase JMJD1A promotes alternative splicing of AR variant 7 (AR-V7) in prostate cancer cells. *Proc. Natl. Acad. Sci. U.S.A.* **115**, E4584–E4593 (2018).